Expression Analysis and Transcription Factor Prediction of Fibroblast Growth Factor 10 During Differentiation of Rat L6 Myoblasts

Shuying FU[1,2], Yifei HUANG[1], Gaojian LI[1], Changseng LI[1], Zhiyin DONG[1], Zilan YANG[1], Qiuyu SONG[1], Jingwen ZENG[1], Yu MEN[1,2], Meiying FENG[1,2]*

1. School of Life Sciences, Zhaoqing University, Zhaoqing 526061, China; 2. Key Laboratory for Research and Utilization of Southern Medicine, Zhaoqing University, Zhaoqing 526061, China

Abstract [**Objectives**] To characterize the expression pattern of Fibroblast growth factor 10 (FGF10) during the differentiation of rat L6 myoblasts and to identify potential key transcription factors (TFs) regulating its expression through bioinformatics approaches. [**Methods**] Rat L6 myoblasts were induced to differentiate by culturing them in DMEM supplemented with 2% donor horse serum (DHS). Morphological changes were observed using an inverted microscope. Cell samples were collected prior to induction (day 0) and on days 1, 3, 5, and 7 post-induction. The relative expression levels of FGF10 mRNA and protein at each time point were quantified using RT-qPCR and Western blot analysis, respectively. Furthermore, a 2 000 bp sequence upstream of the transcription start site of the rat *Fgf10* gene was extracted as the promoter region. Putative TF binding sites were predicted using four databases (TRANSFAC, JASPAR, HOCOMOCO, and CISBP), and high-confidence candidates were screened to construct a regulatory network. [**Results**] Morphological observations confirmed successful differentiation, as evidenced by the appearance of binucleated myotubes on day 3 and the formation of numerous thick, multinucleated myotubes by day 7. Both RT-qPCR and Western blot analysis demonstrated a significant dynamic expression pattern of FGF10. Expression levels were markedly upregulated during the early phase (days 1 - 3), reaching a peak on day 3 ($P < 0.01$), followed by a decline to basal levels during the late phase (days 5 - 7). Cross-validation across multiple databases identified 48 high-confidence TFs, among which *Elf5*, *Tcf3*, *Nkx3-2*, *Zic2*, *Tcf7*, and *Egr1* were consistently predicted by all four databases. [**Conclusions**] FGF10 exhibits high expression levels during the early stage of differentiation, indicating its crucial role in the initiation of myogenesis. The six identified TFs serve as core candidate regulators of *Fgf10* expression, offering novel insights into the molecular mechanisms underlying muscle development.

Key words L6 myoblast, Differentiation, FGF10, Transcription factor, Expression pattern

0 Introduction

Skeletal muscle, one of the most abundant tissues in vertebrates, not only endows the organism with locomotor capabilities but also serves as a critical hub for maintaining whole-body protein turnover and metabolic homeostasis[1]. In the livestock industry, the extent of skeletal muscle development, along with the microstructure and physicochemical properties of muscle fibers, directly determine core economic indicators such as meat yield, tenderness, and juiciness[2]. Consequently, it remains a primary focus of genetic breeding and nutritional regulation. From the perspective of developmental biology, skeletal muscle formation, or myogenesis, is a continuous process that is strictly orchestrated in space and time[3]. Initiated from myogenic progenitor cells during embryogenesis, this process is driven by a cascade of myogenic regulatory factors[4-5]. These cells undergo proliferative expansion, then exit the cell cycle in a controlled manner, initiate specific differentiation programs, fuse to form multinucleated myotubes, and ultimately mature into contractile muscle fibers. Among these stages, myoblast differentiation is regarded as a critical process that determines both the total number and the compositional types of muscle fibers. The efficiency of this differentiation not only directly influences final muscle mass but is also closely linked to the regenerative capacity following muscle injury[6]. Although current scientific research has established the basic molecular framework of skeletal muscle development, given the complexity of the extracellular microenvironment and intracellular signaling networks, deeply elucidating the specific regulatory mechanisms of signaling molecules during the initiation and progression of myoblast differentiation remains a vital task for deciphering muscle biology and identifying genes related to superior traits.

The Fibroblast growth factor (FGF) family comprises a diverse group of polypeptide growth factors that regulate various biological processes, including cell proliferation, differentiation, and organogenesis, by activating specific receptor-mediated signaling pathways. FGF10, a key paracrine factor within this family, has been shown to play significant roles in the morphogenesis of various organs such as the limbs, lungs, and heart[7-8]. In muscle

Received: December 15, 2025 Accepted: January 18, 2026
Supported by Guangdong Basic and Applied Basic Research Foundation (2023A1515110973); Guangdong Provincial Young Innovative Talents Project of General Colleges and Universities (2023KQNCX089); Key Field Special Project of Guangdong Provincial Colleges and Universities (2025ZDZX2077); the Rural Science and Technology Commissioner Program of Guangdong Province (KTP20240673); Undergraduate Higher Education Teaching Quality and Reform Projects of Guangdong Province (Yuejiao Gao Han[2024]No. 9; Yuejiao Gao Han[2024] No. 30); Zhaoqing Science and Technology Innovation Guidance Project (Zhaoke[2025] No. 4); Scientific Research Foundation of Zhaoqing University (QN202436); College Student Innovation Training Program Project (S202510580042).
Shuying FU, doctoral degree, lecturer, research fields: gene function and bioinformatics. * Corresponding author. Meiying FENG, doctoral degree, associate professor, research fields: reproductive physiology and biotechnology.

tissue research, existing evidence suggests that FGF10 plays a role in regulating the proliferation and differentiation of myoblasts, thereby influencing overall skeletal muscle development[9-10]. However, the specific temporal expression patterns of FGF10 during myoblast differentiation, as well as the specific transcription factors (TFs) that regulate its gene promoter region, have been relatively underexplored. The precise mechanisms by which FGF10 functions in skeletal muscle differentiation require further exploration.

Therefore, this study utilized rat L6 myoblasts as an *in vitro* model[11]. A differentiation induction system was established, and RT-qPCR along with Western blot analysis were conducted to assess changes in FGF10 expression during myoblast differentiation. Concurrently, bioinformatics approaches were used to analyze the promoter sequence of the *Fgf10* gene and to predict potential TFs regulating its expression. This study aims to characterize the expression pattern of FGF10 during the differentiation of L6 cells and to conduct a preliminary screening for potential upstream regulators, thereby providing experimental evidence to support future in-depth research into the molecular regulatory networks of FGF10 in skeletal muscle development.

1 Materials and methods

1.1 Materials

1.1.1 Cell line. The rat L6 myoblast cell line was obtained from the Cell Bank of the Chinese Academy of Sciences (Shanghai, China). The cells were tested and confirmed to be free of mycoplasma, bacteria, and fungi. Short tandem repeat (STR) profiling further verified the absence of cross-contamination with human or other species-derived cell lines.

1.1.2 Reagents and antibodies. High-glucose Dulbecco's Modified Eagle Medium (DMEM), donor horse serum (DHS), and 0.25% trypsin-EDTA were purchased from Gibco (USA). Fetal bovine serum (FBS) was obtained from ExCell Bio (Shanghai, China). The UNIQ-10 Column Total RNA Extraction Kit and nitrocellulose (NC) membranes were procured from Sangon Biotech (Shanghai, China). The Reverse Transcription Reagent Kit with gDNA Eraser and qPCR master mix were acquired from Takara (Dalian, China). SDS-PAGE gel preparation kits, RIPA lysis buffer, BCA protein assay kits, blocking buffer, and enhanced chemiluminescence (ECL) reagents were sourced from Beyotime Biotechnology (Shanghai, China). Primary antibodies against FGF10 and GAPDH were obtained from Affinity Biosciences (Wuhan, China). Additionally, the PageRuler Plus Prestained Protein Ladder and HRP-conjugated goat anti-rabbit IgG secondary antibodies were purchased from Thermo Fisher Scientific (USA).

1.2 Methods

1.2.1 Cell culture and differentiation induction. L6 myoblasts were cultured at 37 ℃ in a humidified incubator containing 5% CO_2. Cells between passages 2 and 15 were used for experiments. For routine maintenance and subculturing, cells were maintained in growth medium consisting of high-glucose DMEM supplemented with 10% FBS. When the cells reached 70% – 80% confluence, the culture medium was replaced with differentiation medium composed of high-glucose DMEM supplemented with 2% DHS to induce myogenic differentiation. Differentiation was maintained for 7 d, with the medium being refreshed daily. Morphological changes were observed and recorded using an inverted microscope. Cell samples were collected prior to induction (day 0) and on days 1, 3, 5, and 7 post-induction for subsequent analysis.

1.2.2 RNA extraction and RT-qPCR. Total RNA was extracted from L6 cells using the UNIQ-10 Column Total RNA Extraction Kit according to the manufacturer's instructions. The extracted RNA was dissolved in 0.1% DEPC-treated water and stored at −80 ℃. RNA concentration and purity were assessed using a NanoDrop One spectrophotometer. For cDNA synthesis, 1 μg of total RNA was reverse-transcribed in a 20 μL reaction volume using a reverse transcription kit, following the manufacturer's protocol. Gene-specific primers for qPCR were designed using the NCBI Primer-BLAST tool, as presented in Table 1.

Table 1 Primer sequences for qPCR

Gene	Forward primer (5'-3')	Reverse primer (5'-3')	Product length//bp
Gapdh	CAACTCCCTCAAGATTGTCAGCAA	GGCATGGACTGTGGTCATGA	118
Fgf10	CTCTCTTTTTGGCACCATACAC	CTCAGACATAGTCATCGCTGAT	170

Each qPCR reaction was performed in a total volume of 20 μL, containing 10 μL of 2 × qPCR master mix, 2 μL of cDNA template, 1.6 μL of forward and reverse primers, and 6.4 μL of ddH_2O. Quantitative PCR was conducted with an initial denaturation at 95 ℃ for 30 sec, followed by 40 cycles of denaturation at 95 ℃ for 5 sec and annealing/extension at 60 ℃ for 30 sec. Melt curve analysis was subsequently performed to confirm the specificity of amplification. This procedure involved heating the sample to 95 ℃ for 15 sec, cooling to 60 ℃ for 60 sec, followed by a final heating step at 95 ℃ for 15 sec. All experiments were performed with three biological replicates and three technical replicates. Relative gene expression levels were calculated using the $2^{-\Delta\Delta Ct}$ method, employing *Gapdh* used as the internal reference gene.

1.2.3 Protein extraction and quantification. L6 cells were washed 2 – 3 times with ice-cold PBS and subsequently lysed on ice using RIPA lysis buffer containing protease inhibitors. The lysates were collected and centrifuged at 15 000 × g for 15 min at 4 ℃. The supernatants were collected and used as total protein extracts. Protein concentrations were quantified using a BCA Protein Assay Kit, employing bovine serum albumin (BSA) to generate a standard curve. Protein samples were mixed with loading buffer, denatured at 95 ℃ for 10 min, and stored at −80 ℃.

1.2.4 Western blot analysis. Equal amounts of protein samples were separated by SDS-PAGE and transferred onto NC membranes

using a wet transfer system. The membranes were then blocked with blocking buffer for 30 min at room temperature to prevent non-specific binding. Subsequently, the membranes were incubated overnight at 4 ℃ with primary antibodies specific to FGF10 and GAPDH. Following three washes with Tris-buffered saline containing Tween 20 (TBST) for 10 min each, the membranes were incubated with HRP-conjugated secondary antibodies for 1 h at room temperature. After additional three washes with TBST, protein bands were visualized using an ECL kit and an automated chemiluminescence imaging system.

1.2.5 Prediction of TFs and network construction. The genomic sequence of the specific transcript for the rat *Fgf10* gene was retrieved from the NCBI RefSeq database. A region extending 2 000 bp upstream of the transcription start site was extracted as the potential promoter sequence. To comprehensively identify putative upstream regulators, a multi-source cross-validation strategy was employed. TF binding sites were predicted by scanning promoter sequences using Position Weight Matrices (PWMs) derived from four major databases: TRANSFAC, JASPAR, HOCOMOCO, and CISBP. To minimize false positives inherent in single-source predictions, a stringent consensus filtering criterion was employed, whereby only TFs identified in at least three of the four databases were considered high-confidence candidates. Finally, the regulatory network representing the interactions between the selected TFs and *Fgf10* was constructed and visualized using Cytoscape software.

1.3 Statistical analysis All experimental data were presented as mean ± standard error of the mean (SEM). Statistical analyses and graphical representations were performed using GraphPad Prism software. Differences between groups were analyzed using one-way analysis of variance (ANOVA), followed by Tukey's post-hoc test for multiple comparisons. Different uppercase letters indicate significant differences at $P<0.05$, whereas distinct lowercase letters indicate significant differences at $P<0.01$.

2 Results and analysis

2.1 Establishment of the rat L6 myoblast differentiation model Rat L6 myoblasts exhibited adherent growth in complete medium. Microscopic observation revealed that the cells were mononucleated and exhibited spindle-shaped, triangular, or polygonal morphologies (Fig. 1). Upon reaching 70% – 80% confluence, the culture medium was replaced with differentiation medium containing 2% horse serum to induce myotube formation. On day 1 of induction, L6 myoblasts initiated contact with one another, with a small proportion of cells undergoing apoptosis. By day 3, the cells exhibited a more ordered and directional arrangement, and some myoblasts had fused to form short, binucleated myotubes. By day 5, the majority of L6 cells had fused and differentiated into multinucleated myotubes. By day 7, these cells underwent further fusion and differentiation, resulting in the formation of thick, branched myotubes, which indicates successful induction of differentiation. Multiple nuclei within the myotubes were clearly observable under the microscope.

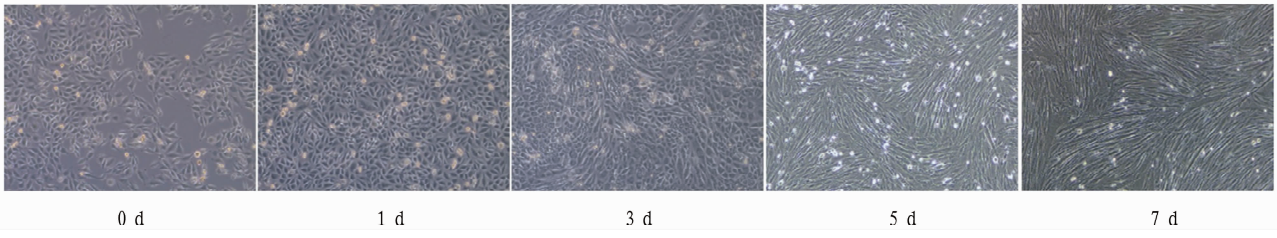

Fig. 1 Morphological changes during induced differentiation of L6 myoblasts (100 ×)

2.2 Expression pattern of *Fgf10* mRNA during the differentiation of rat L6 myoblasts To investigate the role of *Fgf10* in the differentiation of L6 myoblasts, the relative mRNA expression levels at various stages of differentiation (days 0, 1, 3, 5, and 7) were quantified using RT-qPCR, with *Gapdh* serving as the internal control. The results revealed a dynamic expression pattern, characterized by an initial increase followed by a subsequent decrease (Fig. 2). Compared to undifferentiated cells (day 0), the relative mRNA level of *Fgf10* was significantly upregulated on day 1 of differentiation ($P<0.01$). Its expression peaked on day 3, reaching approximately 9-fold higher than that of the undifferentiated group, and was significantly elevated relative to all other time points ($P<0.01$). Thereafter, *Fgf10* mRNA levels began to decline, and by day 5, they were significantly lower than those observed on day 1 ($P<0.05$) and day 3 ($P<0.01$). By day 7, its expression had returned to basal levels comparable to those prior to differentiation. These findings indicate that the transcription of *Fgf10* is dynamically regulated during L6 cell differentiation, exhibiting a transient upregulation in the early phase. This observation suggests that FGF10 may play a critical regulatory role, particularly during the early stages of myoblast differentiation.

2.3 Expression pattern of FGF10 protein during the differentiation of L6 myoblasts To determine whether the transcriptional changes in *Fgf10* corresponded to alterations at the protein level, the abundance of FGF10 protein during L6 cell differentiation was quantified via Western blot analysis. The results showed that the expression pattern of the FGF10 protein was largely consistent with the dynamic trend observed at the mRNA level (Fig. 3). In undifferentiated L6 cells (day 0), the FGF10 protein level was low. Following the induction of differentiation, its expression began to increase on day 1 and peaked on day 3. Subsequently, the FGF10 protein level gradually declined during the later stages of differentiation (days 5 and 7). These findings confirm that FGF10 protein expression is significantly upregulated in the early phase of

L6 cell differentiation. This observation aligns with the RT-qPCR results, and collectively, these results strongly suggest that FGF10 plays a crucial role in the initial stages of myogenesis.

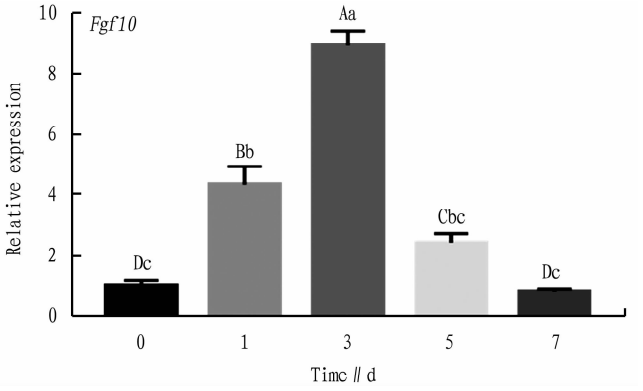

NOTE Different uppercase letters indicate significant differences at $P < 0.05$, and different lowercase letters indicate significant differences at $P < 0.01$.

Fig. 2 Relative *Fgf10* mRNA expression levels during the differentiation of L6 myoblasts into myotubes

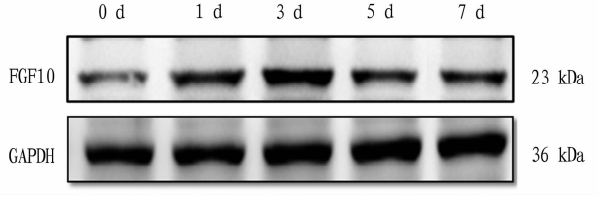

Fig. 3 Protein expression changes of FGF10 during the differentiation of L6 myoblasts into myotubes

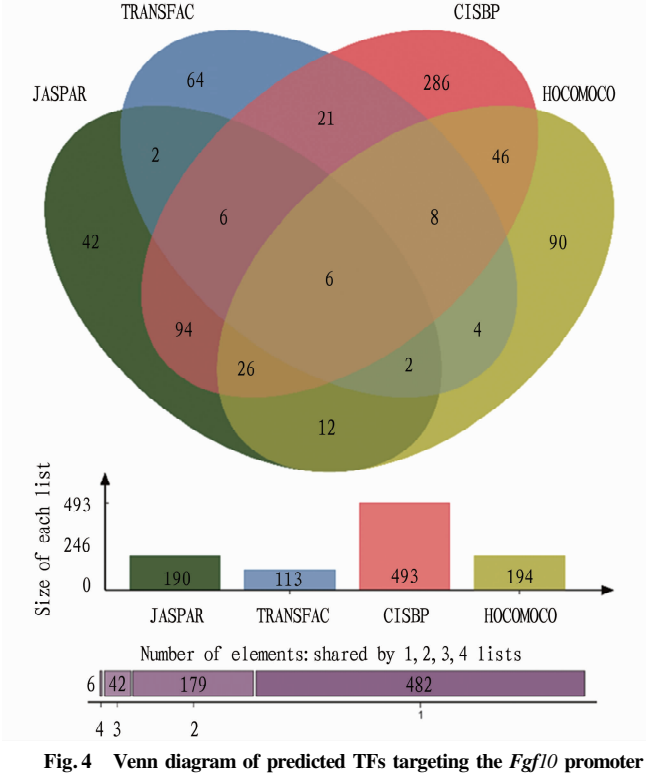

Fig. 4 Venn diagram of predicted TFs targeting the *Fgf10* promoter

2.4 Prediction and screening of potential TFs in the *Fgf10* promoter region To elucidate the potential molecular mechanisms regulating *Fgf10* during L6 myoblast differentiation, putative TF binding sites were predicted within the 2 000 bp region upstream of the transcription start site of the *Fgf10* gene. Four major databases were utilized for this analysis, including JASPAR, TRANSFAC, CISBP, and HOCOMOCO. As illustrated in Fig. 4, the prediction results yielded 190, 113, 493, and 194 TFs from each respective database. After eliminating duplicates, a total of 709 unique TFs were obtained. Intersection analysis identified 179 TFs predicted by two databases, 42 predicted by three databases, and only 6 consistently predicted by all four databases. To enhance the reliability of these predictions and refine the candidate list, an *Fgf10*-TFs regulatory network was constructed using factors predicted by at least three databases, obtaining a total of 48 TFs (Fig. 5). Within the network, the six TFs predicted by all four databases, specifically *Elf5*, *Tcf3*, *Nkx3-2*, *Zic2*, *Tcf7*, and *Egr1*, are highlighted in red, suggesting that they may serve as key candidate regulators of *Fgf10* expression.

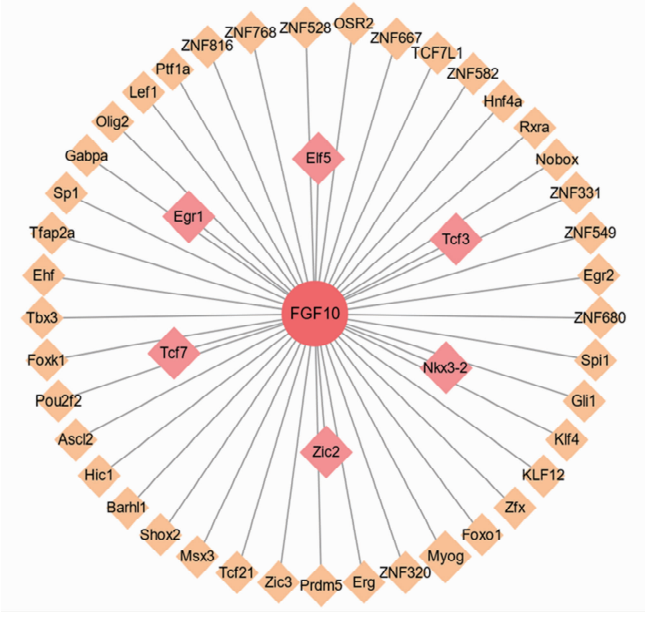

NOTE The network was constructed using TFs predicted by at least three databases. Red nodes represent the six key candidate TFs (*Elf5*, *Tcf3*, *Nkx3-2*, *Zic2*, *Tcf7*, and *Egr1*) predicted by all four databases.

Fig. 5 Regulatory network of *Fgf10* and putative TFs

3 Discussion

The development and repair of skeletal muscle rely on the precise transition of myoblasts from a proliferative state to a differentiated state, a process accompanied by significant morphological changes and the activation of specific gene programs[12]. In this study, an *in vitro* differentiation model was successfully established using rat L6 myoblasts, observing cell fusion and the formation of multinucleated myotubes under low-serum induction, which

aligns with typical characteristics of myogenic differentiation. Within this model, both mRNA and protein expression levels of FGF10 exhibited a dynamic pattern characterized by an initial increase followed by a subsequent decrease, peaking on day 3 of differentiation. The observed expression pattern suggests that FGF10 is not uniformly expressed throughout the process but exhibits a distinct temporal specificity. The significant upregulation of FGF10 during the initiation phase (days 1 – 3) implies that it may serve as an early initiation signal involved in cell cycle withdrawal or the onset of fusion in myoblasts. This finding is consistent with several reports indicating that members of the FGF family promote myoblast migration and fusion[13 – 14]. In the late stage of differentiation (days 5 – 7), as myotubes matured and thickened, FGF10 expression rapidly returned to basal levels. This suggests that high levels of FGF10 are no longer required for the maintenance of terminal differentiation, and sustained high expression may even interfere with subsequent muscle fiber maturation. Notably, changes in FGF10 protein levels showed no significant delay and closely corresponded with mRNA levels, indicating that the abundance of FGF10 during myogenesis is strictly regulated primarily at the transcriptional level. Therefore, elucidating the transcriptional regulatory mechanisms within its gene promoter region is essential for understanding the functional role of FGF10.

Although the importance of FGF10 in skeletal muscle is increasingly recognized, the identity of the specific upstream regulators of FGF10 expression has yet to be identified. To address this issue, the present study employed a multi-database intersection strategy to comprehensively analyze the promoter region of the rat *Fgf10* gene. Compared to predictions derived from a single database, TFs identified by the intersection of four databases demonstrate greater reliability. This study identified six core candidate TFs: *Elf5*, *Tcf3*, *Nkx3-2*, *Zic2*, *Tcf7*, and *Egr1*. The identification of these TFs offers significant insights into the mechanisms underlying the peak expression of FGF10. Notably, *Tcf3* and *Tcf7* are well-established effectors within the Wnt signaling pathway[15]. The Wnt signaling pathway is widely recognized as a critical regulator of skeletal muscle development and has been shown to directly induce the expression of myogenic regulatory factors, including MyoD[16 – 17]. Therefore, it is hypothesized that the Wnt signaling pathway may activate FGF10 transcription upstream by directly binding *Tcf3* or *Tcf7* to the *Fgf10* promoter. Additionally, *Egr1* is a typical immediate early gene that responds to various growth signals and regulates cell differentiation. Its inclusion in the prediction list is logically consistent with the elevated expression of FGF10 in the early phase of differentiation[18 – 19]. The appearance of developmental related TFs such as *Nkx3-2* and *Zic2* further suggests that FGF10 expression is orchestrated by a complex developmental signaling network[20 – 21]. These prediction results construct a novel regulatory hypothesis linking TFs, FGF10, and myogenic differentiation, thereby offering specific targets for future experimental verification.

These findings suggest that targeted strategic interventions during specific windows of animal growth, such as the juvenile stage, hold significant application value for livestock production. On the one hand, functional feed additives capable of activating key upstream TFs could be developed. This nutritional approach would endogenously enhance FGF10 expression, thereby promoting skeletal muscle development and improving feed conversion efficiency without the use of exogenous hormones[22 – 23]. On the other hand, the TF binding sites identified in this study provide potential genetic markers for molecular breeding in livestock. Screening for single nucleotide polymorphisms (SNPs) within the *Fgf10* promoter region that affect the binding efficiency of these key TFs could serve as molecular probes for assessing meat production potential, thereby facilitating the selection of superior lines characterized by rapid growth and enhanced muscle mass. Furthermore, since the efficiency of myogenic differentiation is directly correlated with meat tenderness and water-holding capacity, precise regulation of the timing of FGF10 expression may facilitate the optimization of both high lean meat yield and superior meat quality traits, ultimately maximizing the economic benefits of livestock production.

4 Conclusions

In conclusion, this study employed the rat L6 myoblast model to characterize the temporal expression and transcriptional regulation of FGF10 during myogenesis. The findings demonstrate that FGF10 exhibits a dynamic expression pattern, with an initial upregulation peaking on day 3, followed by a subsequent downregulation. These results highlight the pivotal regulatory role of FGF10 in the initiation phase of differentiation rather than in its maintenance. Furthermore, multi-database bioinformatics analysis identified six core upstream TFs including *Elf5*, *Tcf3*, *Nkx3-2*, *Zic2*, *Tcf7*, and *Egr1*, implying that FGF10 transcription is precisely orchestrated by key pathways such as Wnt signaling. These results offer new insights into the transcriptional regulation of skeletal muscle development and present potential molecular targets for enhancing meat yield and quality in livestock.

References

[1] YIN L, LI N, JIA W, *et al*. Skeletal muscle atrophy: From mechanisms to treatments[J]. Pharmacological Research, 2021, 172: 105807.

[2] TIAN Z, YU M, CUI Y, *et al*. Source of dietary iron and zinc affects meat quality by altering muscular fatty acid profile, flavor substances, and metabolomics in finishing pigs[J]. Meat Science, 2025, 225: 109813.

[3] ENGQUIST E N, ZAMMIT P S. The satellite cell at 60: The foundation years[J]. Journal of Neuromuscular Diseases, 2021, 8(s2): S183 – S203.

[4] DUMONT N A, BENTZINGER C F, SINCENNES M C, *et al*. Satellite cells and skeletal muscle regeneration[J]. Comprehensive Physiology, 2015, 5(3): 1027 – 1059.

[5] SOUSA-VICTOR P, GARCIA-PRAT L, MUNOZ-CANOVES P. Control of satellite cell function in muscle regeneration and its disruption in ageing[J]. Nature Reviews Molecular Cell Biology, 2022, 23(3): 204 – 226.

(To page 44)

demic year, such as "Dynamic Monitoring of Smart Cities" or "Emergency Response to Major Natural Disasters." In this process, learning groups are scientifically structured to comprehensively collect key project data and information, integrating acquired knowledge to complete the entire workflow—from data collection and algorithm selection to system development and report writing—thereby effectively assessing students' practical competencies. Students are also encouraged to participate in AI remote sensing competitions during their spare time, demonstrating their learning and exploratory capabilities through competitive engagement, and stimulating innovative potential within both competitive and collaborative contexts. Such practical training effectively lays a solid foundation for later-stage industry-education collaborative cultivation. Universities can establish off-campus remote sensing laboratories and practice bases in partnership with enterprises in the remote sensing technology sector. This process gives rise to a "dual-mentor" teaching model, featuring "on-campus mentors imparting knowledge and off-campus mentors guiding practice", jointly forming a remote sensing AI talent cultivation alliance that achieves seamless alignment between talent development and industrial demands.

3 Conclusions

In summary, the advent of the AI era presents opportunities for deepening reform in Remote Sensing Science and Technology, while simultaneously imposing higher demands on university talent cultivation models. In the near future, as technology continues to advance, the Remote Sensing Science and Technology discipline will undergo dynamic adjustments and iterative evolution in response to the times. This requires educators to innovate their teaching philosophies, enhance their instructional competencies, deepen the integration of industry and education, and cultivate innovative talents in the remote sensing field who can truly lead the future and harness intelligent technologies.

References

[1] HE Y, LIU T, YAN HW, *et al.* Teaching reform and practice in the course of microwave remote sensing in the era of artificial intelligence [J]. Hydrographic Surveying and Charting, 2025, 45(4): 66 – 71. (in Chinese).

[2] SUN YG, NIU ZY, ZHAO JY, *et al.* Exploration and practice of smart classrooms in the era of artificial intelligence: A case study of "Remote Sensing Geoscience Analysis and Applications" [J]. Advances in Social Sciences, 2025,14(8): 308 – 313. (in Chinese).

[3] YAO FQ, NING SX, DU SW, *et al.* Exploration on the Reform of Innovative Talent Training Mode for Remote Sensing Science and Technology Majors Based on OBE Concept [J]. The Theory and Practice of Innovation and Enterpreneurship, 2024(5): 155 – 159. (in Chinese).

[4] JIN YT, ZHU X, YAN XJ, *et al.* Construction and implementation path of local university graduate training mode under the new development concept: Taking Remote Sensing Science and Technology Specialty as an example [J]. Journal of Higher Education, 2025, 11(20): 171 – 174. (in Chinese).

(From page 38)

[6] SCHMIDT M, SCHULER S C, HUTTNER S S, *et al.* Adult stem cells at work: Regenerating skeletal muscle [J]. Cellular and Molecular Life Sciences, 2019, 76(13): 2559 – 2570.

[7] KOOPMANS T, van ROOIJ E. A dualistic approach to heart repair through FGF10 [J]. Cardiovascular Research, 2022, 118(12): 2564 – 2565.

[8] WATSON J, FRANCAVILLA C. Regulation of FGF10 signaling in development and disease [J]. Frontiers in Genetics, 2018, 9: 500.

[9] XU Q, LIN S, WANG Y, *et al.* Fibroblast growth factor 10 (FGF10) promotes the adipogenesis of intramuscular preadipocytes in goat [J]. Molecular Biology Reports, 2018, 45(6): 1881 – 1888.

[10] HAN L, FU R, FU B, *et al.* Integrating metabolomics and transcriptomics to analyze differences in muscle mass and flavor formation in Gayal and yellow cattle [J]. Frontiers in Veterinary Science, 2025, 12: 1581767.

[11] ONUKI Y, NANASHIMA N, SASAKI Y, *et al.* Oxaloacetate and ketone bodies synergistically promote myoblast differentiation in L6 Cells [J]. Molecules, 2025, 30(10): 2101.

[12] CHAL J, POURQUIÉ O. Making muscle: skeletal myogenesis *in vivo* and *in vitro* [J]. Development, 2017, 144(12): 2104 – 2122.

[13] HAN D, ZHAO H, PARADA C, *et al.* A TGFβ-Smad4-Fgf6 signaling cascade controls myogenic differentiation and myoblast fusion during tongue development [J]. Development, 2012, 139(9): 1640 – 1650.

[14] PAWLIKOWSKI B, VOGLER T O, GADEK K, *et al.* Regulation of skeletal muscle stem cells by fibroblast growth factors [J]. Developmental Dynamics, 2017, 246(5): 359 – 367.

[15] OMBRATO L, LLUIS F, COSMA M P. Regulation of self-renewal and reprogramming by TCF factors [J]. Cell Cycle, 2012, 11(1): 39 – 47.

[16] ZHANG X, HE L, WANG L, *et al.* CLIC5 promotes myoblast differentiation and skeletal muscle regeneration via the BGN-mediated canonical Wnt/β-catenin signaling pathway [J]. Science Advances, 2024, 10(41): eadq6795.

[17] WANG M, YANG J, WU Y, *et al.* Curcumin-activated Wnt5a pathway mediates Ca^{2+} channel opening to affect myoblast differentiation and skeletal muscle regeneration [J]. Journal of Cachexia, Sarcopenia and Muscle, 2024, 15(5): 1834 – 1849.

[18] BAEK J, LOPEZ P A, LEE S, *et al.* Egr1 is a 3D matrix-specific mediator of mechanosensitive stem cell lineage commitment [J]. Science Advances, 2022, 8(15): eabm4646.

[19] ZHANG W, TONG H, ZHANG Z, *et al.* Transcription factor EGR1 promotes differentiation of bovine skeletal muscle satellite cells by regulating *MyoG* gene expression [J]. Journal of Cellular Physiology, 2018, 233(1): 350 – 362.

[20] PAN H, GUSTAFSSON M K, ARUGA J, *et al.* A role for Zic1 and Zic2 in Myf5 regulation and somite myogenesis [J]. Developmental Biology, 2011, 351(1): 120 – 127.

[21] CAIRNS D M, LIU R, SEN M, *et al.* Interplay of Nkx3.2, Sox9 and Pax3 regulates chondrogenic differentiation of muscle progenitor cells [J]. PloS One, 2012, 7(7): e39642.

[22] POSEY E A, DAVIS T A. Review: Nutritional regulation of muscle growth in neonatal swine [J]. Animal, 2023, 17 Suppl 3(Suppl 3): 100831.

[23] RIMMER L A, GEISBRECHT E R, CHAO M D, *et al.* Skeletal muscle metabolism is dynamic during porcine postnatal growth [J]. Metabolites, 2024, 14(7): 357.